



PERGAMON

International Journal of Heat and Mass Transfer 44 (2001) 3213–3222

International Journal of  
**HEAT and MASS  
TRANSFER**

www.elsevier.com/locate/ijhmt

# Mass transfer process during the $\text{NaClO}_3$ crystal growth process

Q. Kang <sup>\*</sup>, L. Duan, W.R. Hu

*National Microgravity Laboratory, Institute of Mechanics, CAS, No. 15 Zhong Guan Cun Road, Beijing 100080, People's Republic of China*

Received 10 July 2000; received in revised form 7 November 2000

## Abstract

Particle image velocimetry (PIV) technology was used directly to measure the convection pattern in sodium chlorate ( $\text{NaClO}_3$ ) crystal growth. The two-dimensional velocity distributions in the solution of  $\text{NaClO}_3$  have been obtained from experiments, and the velocity fields were compared with concentration fields that have been obtained by a phase-shift interferometer. The structures of both results of the velocity fields and concentration fields agree well. The coupling action of velocity and concentration was analyzed. © 2001 Elsevier Science Ltd. All rights reserved.

*Keywords:* Crystal growth; Buoyancy convection; Mass transfer; PIV; Interferometer

## 1. Introduction

In the crystal growth process from solution, the characteristics of flow field outside the crystal are important factors affecting both the growth rate and the quality of crystal. The property of the crystal depends highly on the solution concentration distribution on the growth surface of a crystal. However, the concentration distributions are affected by the diffusion and convection of the solution. On the ground, the convections caused by buoyancy are generally unavoidable in the crystal growth process from solution. Firstly, a concentration field is a direct factor affecting crystal growth. On the other hand, spatial variety of concentration field could induce the convection of solution outside the crystal due to the buoyancy effect. Furthermore, the convection of solution could change the spatial distribution of concentration. The interaction of concentration field and velocity field is a complex problem. The two actions are coupled with each other.

The optical technique that is non-destructive and for whole flow field has been widely used to study the process of crystal growth experimentally. However, most works gave only simple character parameters and a few qualitative analyses results [1–3], such as the thickness of the diffusion boundary layer and the possibility of buoyancy convection. The information dealing with the whole field concentration distribution and velocity distribution together with the process of the crystal growth and the fluid dynamics idea are few experimentally.

For understanding and visualizing the flow pattern and concentration distribution in the transparent solution, the concentration distributions have been measured by using a Mach–Zehnder interferometer and the velocity field was measured by using particle image velocimetry (PIV) in the present experiment. The velocity field, concentration field and their relations are analyzed thereby.

It is very significant to study the concentration distribution and velocity distribution by the experimental method, since could it not only help us understand the relation of crystal growth with outside field directly, but also it may provide the data to analyze theoretically the interaction of concentration field and velocity field by fluid dynamics method.

<sup>\*</sup> Corresponding author. Fax: +86-10-62561284.  
E-mail address: kq@mail.imech.ac.cn (Q. Kang).

Nomenclature		$Ra$	Rayleigh number
$C$	concentration of solution	$Ra_c$	critical Rayleigh number
$C_o$	concentration of solution located on the surface of a crystal	<i>Greek symbols</i>	
$C_\infty$	concentration of solution in far field	$\alpha$	concentration gradient
$d$	characteristic length	$\beta_C$	solubility expansion coefficient
$D$	solute diffusion coefficient	$\Delta C$	concentration difference of solution
$g$	gravitational acceleration	$\Delta n$	refractive index difference
$n$	refractive index	$\nu$	kinematic viscosity coefficient

## 2. The experiment model

In the present experiment, the crystal growth cell is a container with a rectangular cross-section of  $20.0 \times 12.0 \text{ mm}^2$  and  $14.0 \text{ mm}$  high. The lateral walls of the container consist of transparent K9 optical glass for optical interferometer measurement and PIV application. The temperature of the growth cell is controlled. The cell is partly filled with  $\text{NaClO}_3$  solution, for which the top boundary at  $10 \text{ mm}$  in height is a free surface.

A seed crystal was put into the growth cell of  $\text{NaClO}_3$  solution at  $21^\circ\text{C}$  at the beginning of the experiment. The initial concentration of  $\text{NaClO}_3$  solution is  $46.43\%$ , which is an undersaturated solution at  $21^\circ\text{C}$ . Because the solution is undersaturated, the seed crystal is dissolved at an early stage. The concentrations of the solution around the crystal would be larger than that far away from the crystal. With the dissolution of the crystal and the decline of the temperature in the solution of growth cell, the concentration of solution would reach its saturation near  $20^\circ\text{C}$ . In this case, the concentration gradient is very small in the solution around the  $\text{NaClO}_3$  crystal. In very short period, the crystal does not dissolve further, neither does the crystal grow in the present experiment. While the temperature of the growth cell keeps on falling gradually at the rate of  $0.5^\circ\text{C}/\text{h}$ , the solution would be in its super-saturation state. Thus, the solution crystallizes gradually on the surface of the seeding crystal and forms a concentration gradient around the crystal. The concentration of the solution around the crystal is smaller than that far away from the crystal.

The buoyancy-driven convection in gravitation field is a typical question of fluid mechanics. The asymmetry

of the temperature (or/and concentration) could bring the asymmetry of the fluid density. The fluid whose density is lower would move to the direction that opposed the gravitational direction, due to the buoyancy effect. The convection will occur in the fluid if the buoyancy is large enough to overcome the viscous resistance and thermal diffusion effect (or/and concentration diffusion effect). According to fluid dynamics theory, there is a dimensionless quantity associated with buoyancy, the Rayleigh number,  $Ra$ , that takes a critical value at the onset of instability. The Rayleigh number for mass convection caused by concentration gradient is defined as [4].

$$Ra = \frac{g\beta_C\alpha d^4}{\nu D}, \quad (1)$$

where  $g$  is the gravity acceleration,  $\beta_C$  is the solubility expansion coefficient,  $\alpha$  is concentration gradient,  $\nu$  is the kinematic viscosity coefficient,  $D$  is the solute diffusion coefficient, and  $d$  is characteristic length. Usually, if the lower boundary surface is a rigid conductor and the air above the liquid layer is considered as an insulating top boundary, linear theoretical analysis gives a critical Rayleigh number  $Ra_c = 669$  for onset of convection in case of absent capillary effect [4].

The physical properties and operating condition of the  $\text{NaClO}_3$  solution used in the present experiment are listed in Table 1. According to the parameters, the concentration Rayleigh number is  $2207$ , which is larger than the above-mentioned critical Rayleigh number. Therefore, the convection of solution should occur in the locale around the crystal when the experiments were done on the ground. However, the convection would vanish in the space experiments. The diffusion process is

Table 1  
The physical properties and operating condition of the  $\text{NaClO}_3$  solution

$\beta_C$ ( $\text{mol}^{-1}$ )	$\nu$ ( $\text{cm}^2 \text{ s}^{-1}$ )	$D$ ( $\text{cm}^2 \text{ s}^{-1}$ )	$\Delta C$ ( $\text{mol}/\text{l}$ )	$d$ ( $\text{cm}$ )
$5.5 \times 10^{-2}$	$1.3 \times 10^{-2}$	$1.5 \times 10^{-5}$	$4.8 \times 10^{-2}$	$5.5 \times 10^{-2}$

a typical phenomenon of mass transfer. Pure diffusion process is a very good condition to make materials, and the new material will come up in the future to be prepared and tested in microgravity environment.

### 3. Diagnostic method

#### 3.1. Particle image velocimetry for velocity field

The PIV has been recently used as a powerful tool for measuring the velocity field in the experiments of fluid mechanics, and it records the flow structure in a cross-section simultaneously. The trace particles should be used in the fluid, and they might influence the process of the crystal growth. The principle of PIV requires to illuminate a cross-section by using a pulse laser light sheet for flow field measured, to record the sequence of the particles images by using a CCD camera (or a film), and to use the image matching method of a sub-area template between two frames obtained the displacement (or velocity) at the each sub-area [5].

A system of digital particle image velocimetry (DPIV) of DANTEC measurement technology A/S with FlowMap PIV 2000 Processor was used to quan-

titatively measure the 2D velocity field in a vertical cross-section of the cell during the process of the crystal growth, as shown in Fig. 1. An argon ion laser was applied to illuminate the flow field. Pulse lights were shaped by an electro-optical shutter, which was controlled by a center processor with CCD camera synchronization. The resolution of CCD camera is  $768 \times 484$  pixels with  $11.6 \times 13.6 \mu\text{m}$  pixel pitch. The silver-coated hollow glass spheres of  $10 \mu\text{m}$  in diameter as tracer particles are suspended in the  $\text{NaClO}_3$  solution. The density of the particles is  $1.4 \text{ g/cm}^3$ , which is close to the density of  $\text{NaClO}_3$  solution. By using a cycling lens, a 1.0 mm thin light sheet is shaped to illuminate a vertical cross-section at the center part of the container. This cross-correlation technique of DPIV image matching processing was used to obtain both magnitude and direction of velocity vector at the same time [6].

Fig. 2 shows the arrangement of PIV set up in the present experiment.

#### 3.2. Laser interferometry for concentration field

In order to obtain the concentration distribution of solution, a Mach-Zehnder interferometry with a phase-shift servo system was used. The interferometry

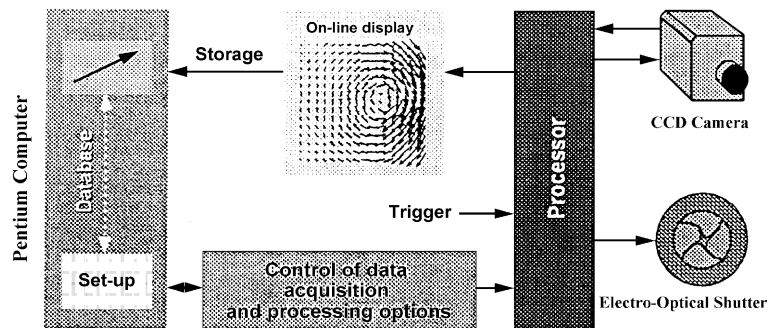


Fig. 1. Schematic block diagram of DPIV system.

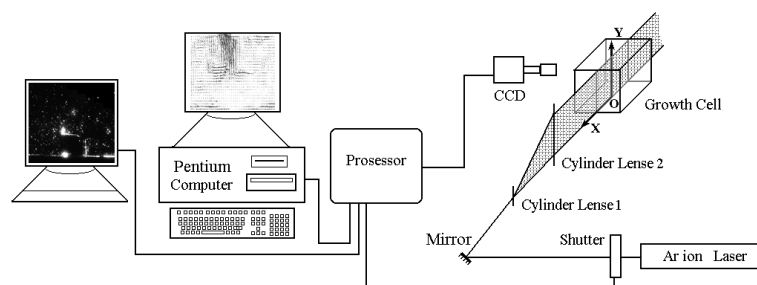


Fig. 2. Arrangement of PIV in the experiment.

Table 2  
The dependency of refractive index on concentration (for  $\text{NaClO}_3$ , at  $20.0^\circ\text{C}$ )

No.	1	2	3	4	5	6	7	8	9
Concentration (mol/l)	0.50	0.75	1.00	1.25	1.5	1.75	2.0	2.25	2.50
Refractive index	1.3445	1.3461	1.3492	1.3512	1.3554	1.3580	1.3594	1.3631	1.3656

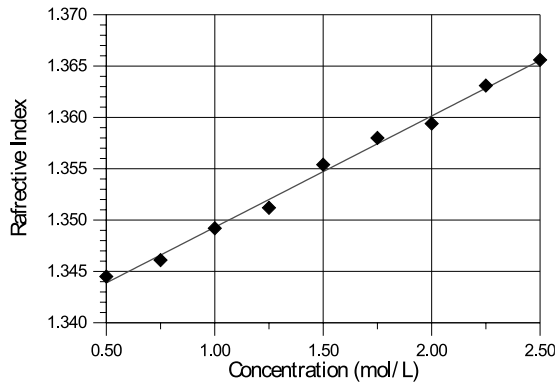


Fig. 3. The relationship curve between refractive index and concentration (for  $\text{NaClO}_3$  solution).

theory and experiment method have been introduced by Duan and Shu [7]. Interference patterns were recorded directly by a computer via a CCD camera.

Refractive index distributions were calculated by using a phase-shift technology and a method of phase unwrapping. The concentration distribution is obtained by using the relationship between the concentration and the refractive index. Method of the recorders and analyses of the interference fringe pattern have also been described in detail by Duan and Shu [7]. Depending on the study of the interference pattern, not only the concentration distributions were obtained but also the existence of the convection phenomena and the modality of the convection pattern were estimated in the process of  $\text{NaClO}_3$  crystal growth although the convection phenomena are not as accurate as the ones given by PIV technology.

The relation between refractive index and concentration of  $\text{NaClO}_3$  solution is an essential parameter to invert the interferometry image to concentration distribution, and was measured by a refractive meter (Type: WAY-15 ABBE Refractometer). The results of measurements are listed in Table 2. The temperature of the  $\text{NaClO}_3$  solution was fixed at  $20.0^\circ\text{C}$  during the

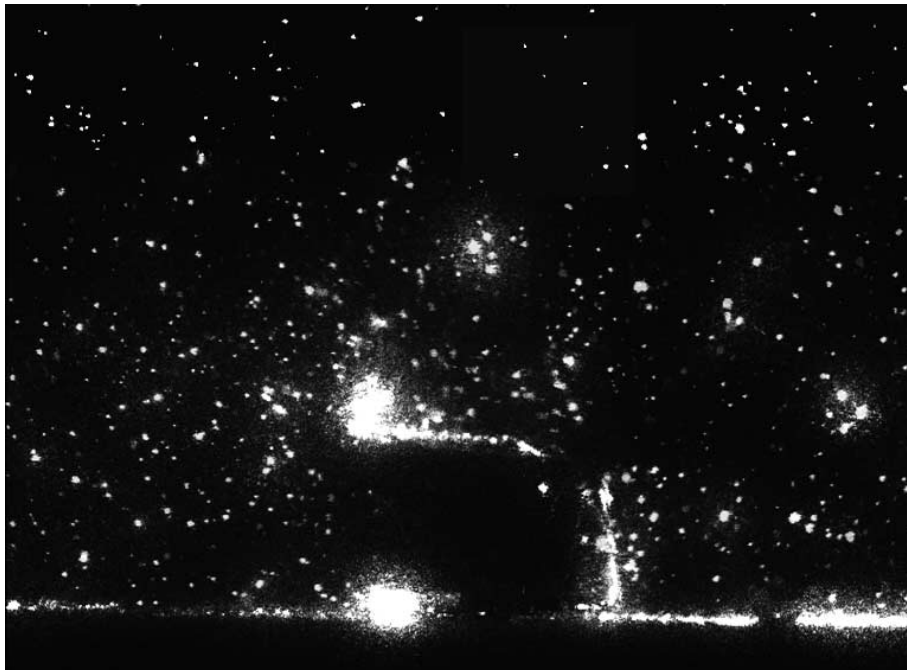


Fig. 4. A particle image of flow field of  $\text{NaClO}_3$  solution.

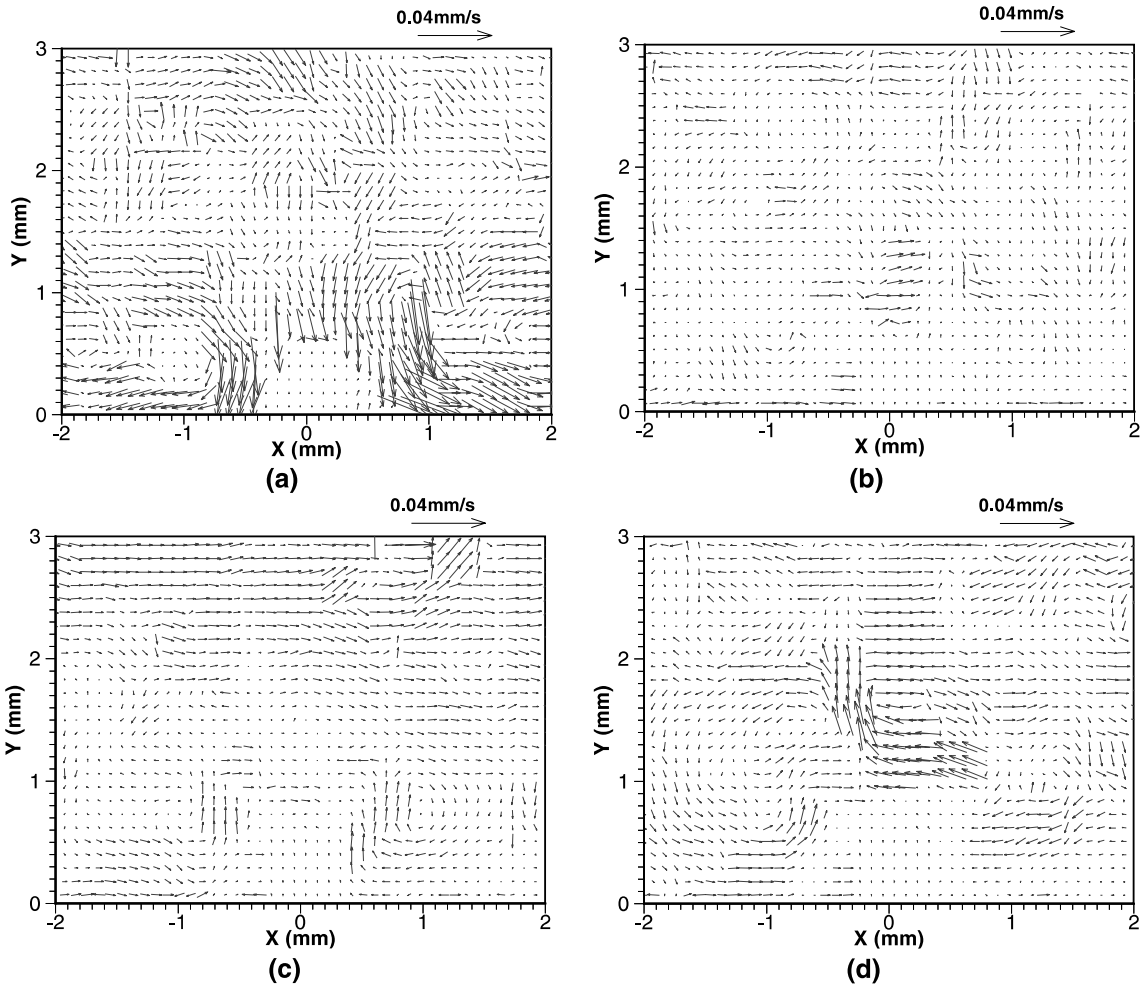


Fig. 5. The evolution of the velocity field.

measurement. Fig. 3 shows the relative curve of the refractive index and concentration by linear fitting, and the relation is found from the linear fitting as:

$$n = 1.33846 + 0.01084C, \tag{2}$$

where  $n$  is the refractive index of  $\text{NaClO}_3$  solution and  $C$  is the mol concentration of  $\text{NaClO}_3$  solution.

The relationship of differential coefficient, or the ratio of refractive index dependence on concentration can be written as follows:

$$\Delta C = 92.25\Delta n. \tag{3}$$

The refraction index dependence on temperature was also studied, and the results show that the refractive index of  $\text{NaClO}_3$  solution is not sensitive to the temperature change within  $5^\circ\text{C}$ .

#### 4. Experimental results with discussion

Fig. 4 shows a particle image of flow field in the solution during the  $\text{NaClO}_3$  crystal growth. The center part on the bottom is a  $\text{NaClO}_3$  seed crystal. Fig. 5 shows the evolution of the velocity field. Figs. 6 and 7 show, respectively, the evolution of the interference pattern and the evolution of the corresponding concentration field. In Fig. 7,  $C$  and  $C_\infty$  are, respectively, the local solution concentration and the solution concentration in far field.

Figs. 6(a) and 7(a) show an interference pattern and a concentration distribution at the early stage of the experiment. Because the solution is undersaturated, the seed crystal is dissolved at this stage. The concentrations of the solution around the crystal are larger than the ones in the solution far away from the

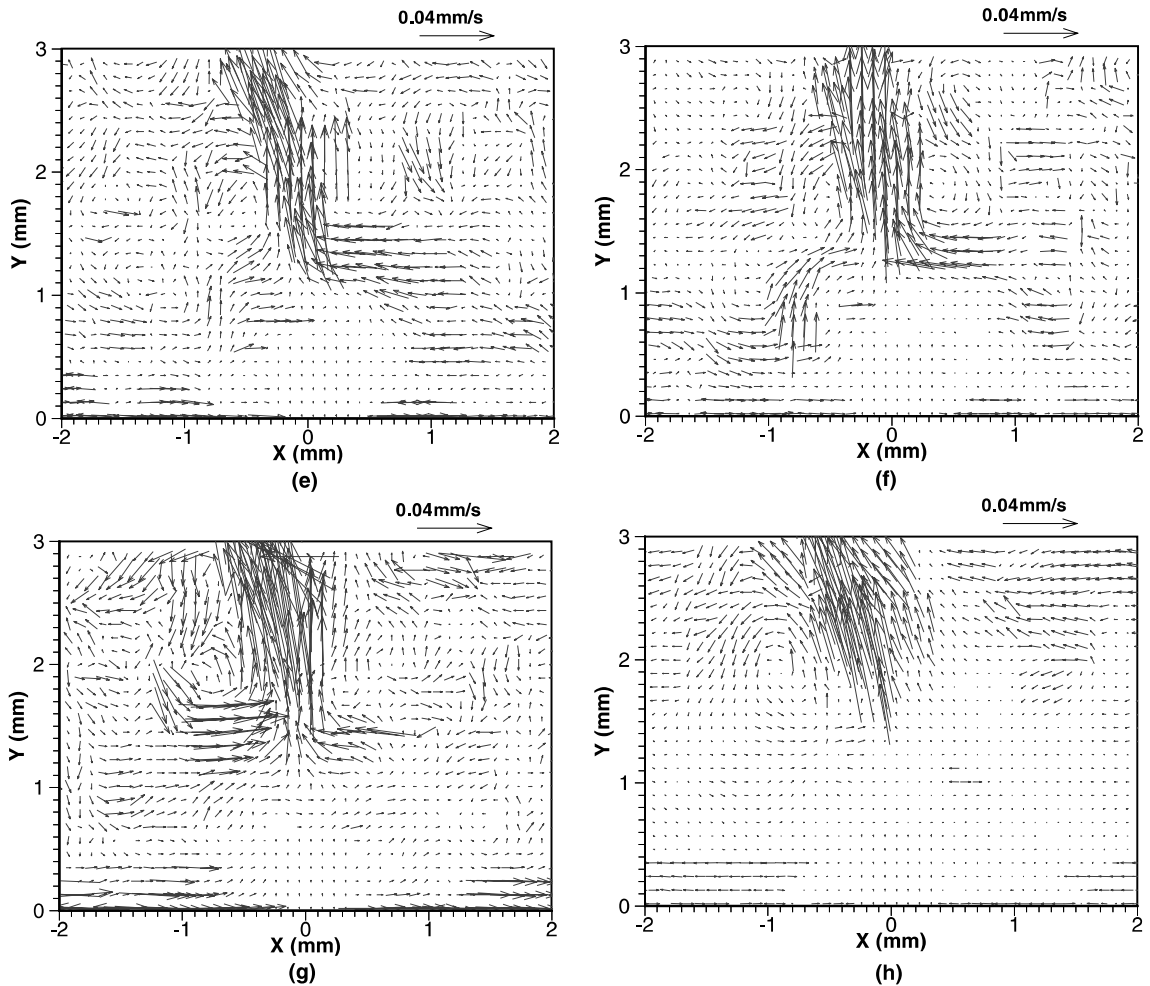


Fig. 5 (continued)

crystal. Due to the existence of the density gradient caused by concentration difference between the upper part of the seed crystal and two sides of the seed crystal, and the direction of the density gradient is opposite to the one of gravity, the solution around the crystal moves downward, as shown in Fig. 5(a), to form a concentration buoyancy flow.

Near the saturation state, the concentration gradient is very small in the solution around the  $\text{NaClO}_3$  crystal, as shown in Figs. 6(b) and 7(b), so that the Rayleigh number would be less than the critical Rayleigh number. Therefore, the convection nearly vanishes, as shown in Fig. 5(b). The concentration delamination caused by gravity can be seen in Figs. 7(a) and (b). It is a very short time period during which the crystal does not dissolve further, and the crystal does not grow in the present

experiment. In this period the convection would also vanish.

At a super-saturation state, the solution crystallizes gradually on the surface of the seeding crystal and forms a concentration gradient around the crystal. The concentration of the solution around the crystal is smaller than that far away from the crystal, as shown in Figs. 6(c)–(h) and 7(c)–(h), and the direction of the density gradient on the top part of the crystal is directly opposite to that of gravity. Hence, the solution in the diffusion boundary layer of the crystal moves upward in the growth cell, and forms a plume flow in the upper part of the crystal, as shown in Fig. 5(c)–(h). We can see from Figs. 7(c)–(h) that the concentration difference around the crystal is gradually increased. The process of velocity increase can be also seen clearly in Fig. 5(c)–(h). The

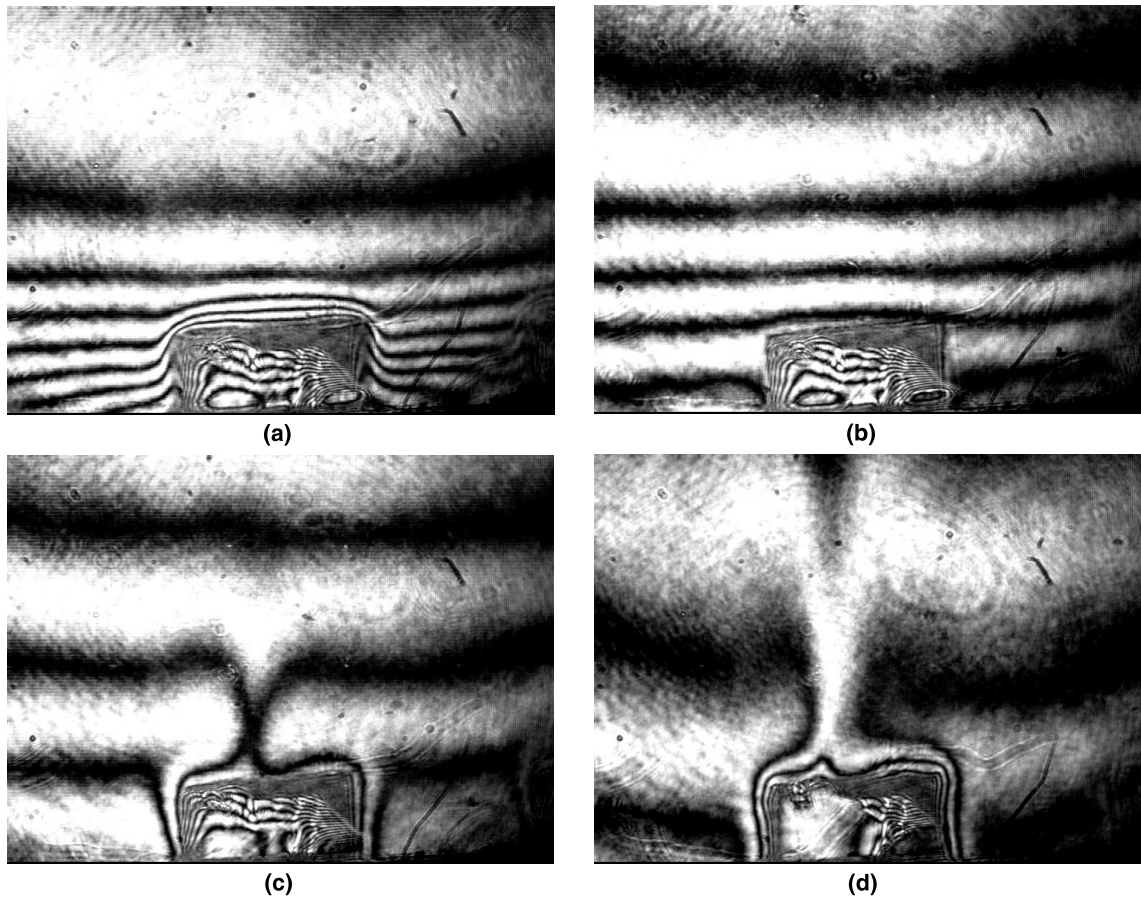


Fig. 6. The evolution of the interference pattern.

flow is still a buoyancy convection driven by the exchange of the concentration under the earth's gravity. The direction of the flow is opposite to that for crystal being dissolved.

These experimental results show clearly that the mass transfer is carried out mainly by the help of the convection caused by the concentration gradient during the period of the crystal growth. However, the concentration gradient would be reduced because of the convection. The coupling processes of concentration and velocity would influence the rate of the crystal growth.

The convection is mainly vertical to the center part of upper crystal face (010) and parallel to the two side crystal faces (100), and the exchange of solution on crystal faces (100) is more plentiful than that on crystal face (010). The concentration difference in the diffusion layer is approximately equal between crystal

face (010) and crystal faces (100) as shown in Fig. 8.  $C$  and  $C_0$  in Fig. 8 are, respectively, the local solution concentration and the solution concentration located on the local surface of the crystal. However, because the thickness of diffusion layer of crystal faces (100) is less than that of crystal face (010), the concentration gradient in the upper part of the crystal is generally less than that near both the sides of the crystal. As shown in Fig. 8, the concentration gradient in the upper part of the crystal is  $0.0085 \text{ mol l}^{-1} \text{ mm}^{-1}$ ; the concentration gradients on both the sides of the crystal are nearly the same as  $0.0120 \text{ mol l}^{-1} \text{ mm}^{-1}$ . Therefore, the mass transfer of crystal faces (100) is more intense than that of crystal face (010), so the growth rate of crystal faces (100) would be faster than that of crystal face (010). The thickness difference of the diffusion boundary layer between crystal face (010) and crystal faces (100) may be caused by the buoyancy convection, not by gravity

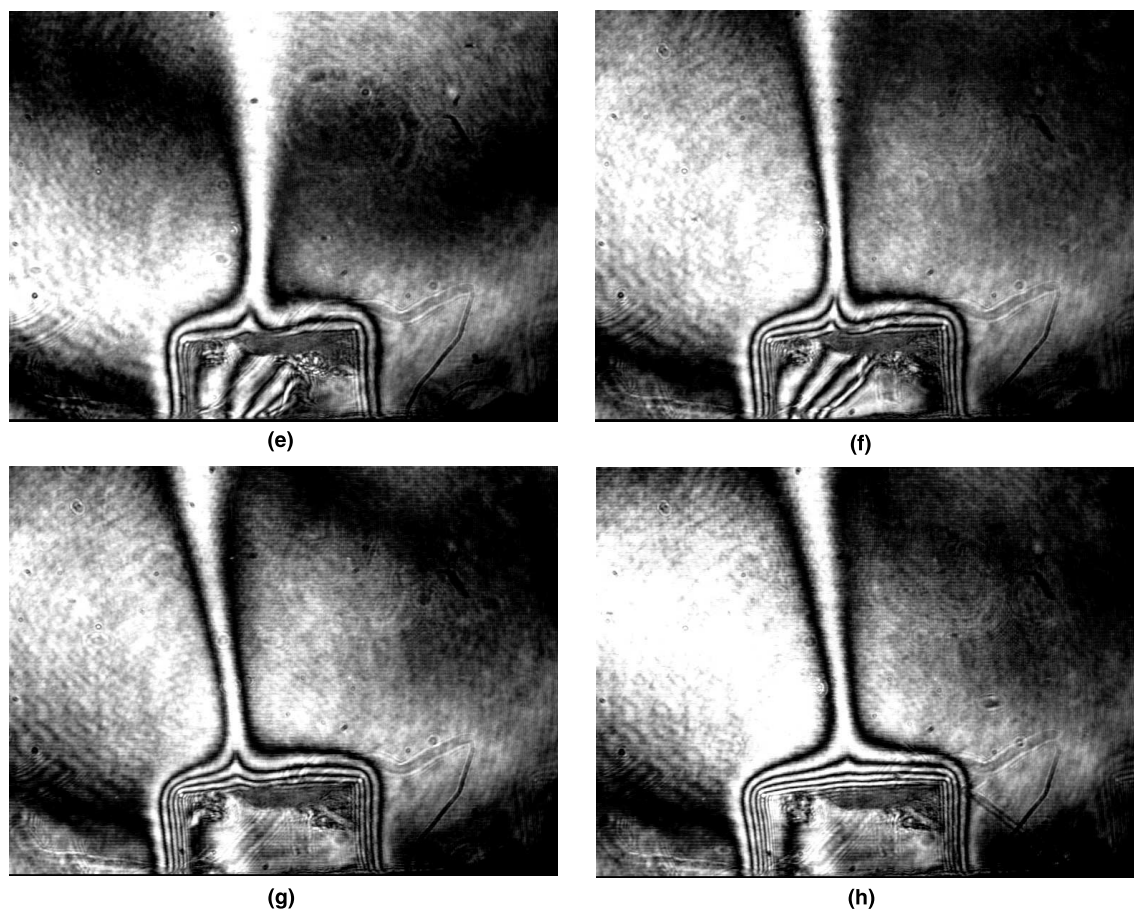


Fig. 6 (continued)

sedimentation. That is, the difference of growth rate between the upper crystal face and the side crystal faces is caused by buoyancy convection. In the microgravity condition, the differences would vanish. The average growth rates of these crystal faces have been given in [7]. The growing diffusion boundary layer is as thick as 350–560  $\mu\text{m}$  as shown in Fig. 8, when the concentration difference is high.

## 5. Conclusions

The PIV and interferometry techniques are for the benefit of understanding the fluid flow phenomena of the crystal growth process and for supporting the observation of the crystal growth together with fluid process. By using the PIV, the velocity fields of  $\text{NaClO}_3$  solution have been acquired successfully. And the concentration fields were also obtained by a Mach–Zehnder interfer-

ometer with phase-shift system. The evolution of flow pattern and interference fringe pattern were recorded during the whole process of both dissolving and crystallizing.

The buoyancy convection phenomena caused by concentration asymmetry are studied in the process of crystal growth. The construction of convection pattern and the construction of concentration pattern were shown clearly. The convection phenomena that were guessed early by analyzing concentration field distribution were confirmed directly by measuring velocity field. The coupling of concentration and velocity were studied thereby. The concentration gradients in the diffusion layer were given quantitatively by analyzing the curve of concentration distribution; and then, the difference of growth rate between crystal faces (100) and crystal face (010) was analyzed. The buoyancy convection (plume flow) during the crystal growth has been visualized and analyzed.



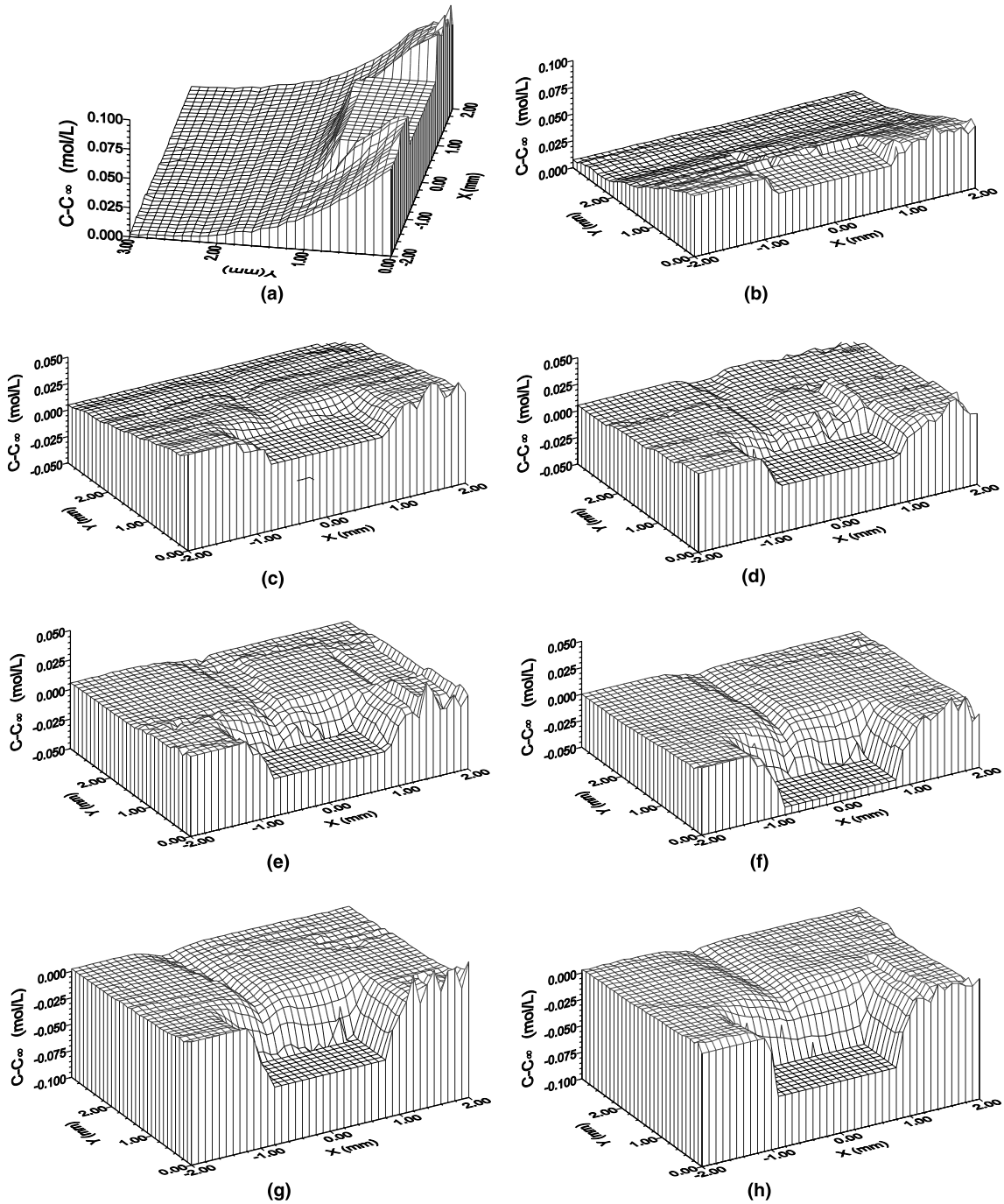


Fig. 7. The evolution of the concentration distribution.

**Acknowledgements**

This research is supported by the grant 95-yu-34 of the Ministry of Sciences and Technology of China,

the grant 19789201 of the National Natural Science Foundation of China, the grant of Rector Foundation of CAS and the Foundation of China Post Doctor.

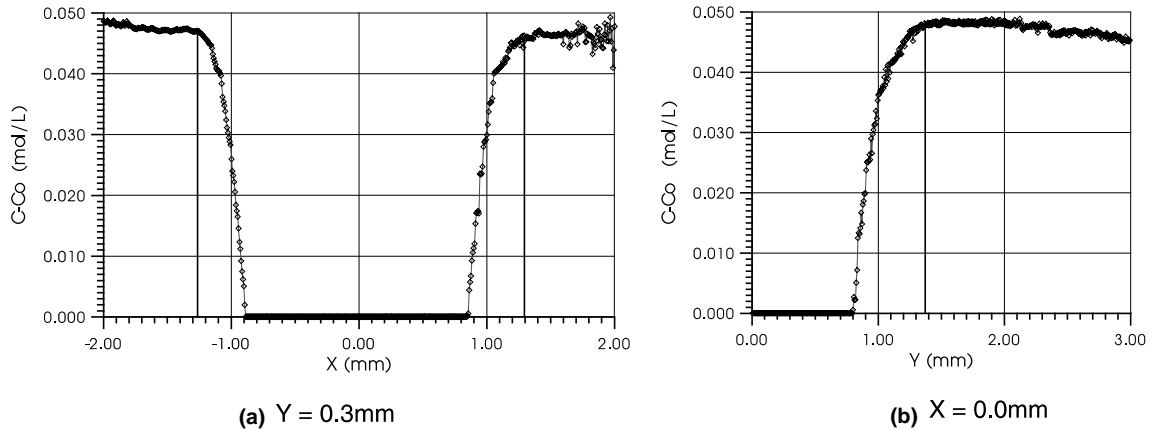


Fig. 8. The concentration curve of the  $\text{NaClO}_3$  solution.

## References

- [1] Kazuo Onuma, Katsuo Tsukamoto, Suezou Nakadate, Application of real time phase shift interferometer to the measurement of concentration field, *J. Cryst. Growth* 129 (1993) 706–718.
- [2] Satoru Miyashita, Hiroshi Komatsu, Yoshihisa Suzuki, et al., Observation of the concentration distribution around a growing lysozyme crystal, *J. Cryst. Growth* 141 (1994) 419–424.
- [3] K. Onuma, K. Tsukamoto, I. Sunagawa, Role of buoyancy driven convection in aqueous solution growth: a case study of  $(\text{BaNO}_3)_2$  crystal, *J. Cryst. Growth* 89 (1988) 177–188.
- [4] D.A. Nield, Surface tension and buoyancy effects in cellular convection, *J. Fluid Mech.* 19 (1964) 341.
- [5] Q. Kang, W.R. Hu, Studies on Bénard–Marangoni convection by PIV, in: *Proceedings of the 47th International Astronautical Congress, AIAA, IAF-96-J.3.10*, 1996.
- [6] *FlowMap Installation & User's guide*, DANTEC Measurement Technology A/S, Denmark, 1996.
- [7] L. Duan, J.Z. Shu, The convection during  $\text{NaClO}_3$  crystal growth observed by real time phase shift interferometry, *J. Cryst. Growth*, in press.